



A method of DEM construction and related error analysis

Chuanfa Chen*, Tianxiang Yue

Institute of Geographical Sciences and Natural Resources Research, Chinese Academy of Sciences, 11A, Datun Road, 3 Anwai, Beijing 100101, China

ARTICLE INFO

Article history:

Received 1 August 2008
Received in revised form
17 November 2009
Accepted 4 December 2009

Keywords:

DEM
Error
Surface modelling
Terrain representation

ABSTRACT

The concept and the computation of terrain representation error (ETR) are investigated and total DEM error is presented as an accuracy index for DEM evaluation at a global level. A promising method of surface modelling based on the theorem of surfaces (SMTS) has been developed. A numerical test and a real-world example are employed to comparatively analyze the simulation accuracy of SMTS and the classical interpolation methods, including IDW, SPLINE and KRIGING performed in ARCGIS 9.1 in terms of sampling and interpolation errors and of total DEM error. The numerical test shows that SMTS is much more accurate than the classical interpolation methods and ETR has a worse influence on the accuracy of SMTS than those of the classical interpolation methods. In a real-world example, DEMs are constructed with SMTS as well as the three classical interpolation methods. The results indicate that, although SMTS is more accurate than the classical interpolation methods, a real-world test indicates that there is a large accuracy loss. Total DEM error composed of, not only sampling and interpolation errors, but also ETRs can be considered as a good accuracy measure for DEM evaluation at a global level. SMTS is an alternative method for DEM construction.

© 2010 Elsevier Ltd. All rights reserved.

1. Introduction

A digital elevation model (DEM) is a numerical representation of topography as a function of geographic location, usually made up of equal-sized grid cells, each with a value of elevation. Its simple data structure and widespread availability have made it a popular tool for land use planning, derivation of geomorphic features, hydrological modelling, large-scale mapping and telecommunications (Fisher, 1993; Gao, 1997; Zhou and Liu, 2004).

DEM, like other spatial data sets, are subject to errors (Fisher and Tate, 2006; Wechsler and Kroll, 2006). Since DEM error can be propagated through GIS operations and affect the quality of final products, it is an important problem to solve (López, 1997). Several factors affect the quality of DEMs (Chaplot et al., 2006). A significant source of error can be attributed to data collection. The accuracy of source data varies with collection techniques, such as map digitization, active airborne sensors, photogrammetric methods and field surveying (Erdogan, 2009). Other sources of error include the interpolation methods for DEM generation and the characteristics of the terrain surface (Carrara et al., 1997; Skidmore, 1989). DEM accuracy assessment is usually undertaken by deriving a measure of DEM accuracy; how close the DEM's elevation values are to the true elevations. Measures such as root mean square error (RMSE) and standard deviation of

the error are frequently used to summarize elevation errors in a DEM at a global level (Bolstad and Stowe, 1994; Carlisle, 2005; Wise, 1998). If GIS users are not aware of the DEM errors, perfectly logical GIS analysis techniques can lead to incorrect results. In other words, the data may not be fit for use in a certain context (Fisher, 1993).

The awareness of the importance of DEM accuracy is shown by the vast number of studies published on the accuracy comparisons of interpolation methods and error detections. For example, Schut (1976) provided an in-depth review of various interpolation techniques used in generating DEMs and the possible DEM errors produced during the data processing. Walsh et al. (1987) found that the total DEM error may be minimized by recognizing both the inherent errors within input products and operational errors created by the combinations of input data. Polidori et al. (1991) introduced the fractal process as a terrain simulation model for improving DEM accuracy. Gao (1998) provided a comprehensive analysis on the impact of sampling schemes on DEM accuracy in constructing DEMs from contour maps and proposed some suggestions for contour digitization. Rees (2000) presented some theoretical and practical assessments of the accuracy of interpolation techniques, with which DEM can be interpolated to higher resolutions. Chaplot et al. (2006) investigated the DEM accuracy estimation in relation to the possible interactions with spatial scale, landform types, and data density based on different interpolation methods. Bonk (2007) determined the effect of input data point designs including random and grid sampling internally varying in number of input data points on the

* Corresponding author. Tel.: +86 10 64889847.
E-mail address: chencf@lreis.ac.cn (C. Chen).

magnitude and spatial distribution of DEM errors. Aguilar et al. (2007) found that the accuracy of the DEM generated from random sampling design is highly correlated with the sampling density.

In order to solve the error problem in surface modelling, a new method of surface modelling based on the theorem of surfaces (SMTS) has been developed. The accuracy of SMTS was assessed in terms of sampling and interpolation errors (Yue et al., 2007). However, potential sources of error may be introduced by the resolution used for surface modelling by interpolation methodology. Previous research (Carter, 1990; Armstrong and Martz, 2003) indicated that DEM resolution plays an important role in terrain representation, and a low resolution can result in a big accuracy loss in complex terrains. Such an accuracy loss is named, terrain representation error (ETR), and the ETR may become a dominant part of the error in a DEM as the grid interval and terrain roughness increases (Chang and Tsai, 1991; Huang and Lees, 2005). Therefore ETR should be taken into account when the accuracy of SMTS and the classical interpolation methods is assessed in terms of error index at a global level.

The rest of this research is organized as follows. First, we introduce the theoretical formulation of SMTS. Second, the concept and the computation of ETR are investigated. Total DEM error is computed in terms of error propagation theorem. Third, two examples including a numerical test and a real-world example are employed to comparatively analyze the simulation accuracy of SMTS and the classical interpolation methods of IDW, SPLINE and KRIGING performed in ARCGIS 9.1 in terms of sampling and interpolation errors and of total DEM error at a global level. At last, some conclusions and discussion are presented.

2. SMTS

According to the fundamental theory of surfaces, a surface is uniquely defined by the first fundamental coefficients and the second fundamental coefficients (Henderson, 1998). The first fundamental coefficients are used to express how the surface inherits the natural inner product of R^3 , in which R^3 is the set of triples (x, y, z) of real numbers (Gray et al., 2006). The coefficients of the first fundamental form of a surface yield some geometric properties of the regions and geodesics on the surface. These geometric properties, that are determined only in terms of the first fundamental coefficients of a surface, are named the intrinsic geometric properties. The collection of these geometric properties forms the subject of the intrinsic geometry of a surface, which indicates that its properties do not depend on the shape of the surface, but depend only on the coefficients of the first fundamental form. The second fundamental form coefficients reflect the local warping of the surface, namely its deviation from tangent plane at the point under consideration (Liseikin, 2004).

Suppose a surface is a graph of a function $z=f(x,y)$ and $\{(x_i,y_j)\}$ is a network created by equally orthogonal division of a computational domain Ω , finite difference of SMTS can be formulated as (Yue et al., 2007),

$$\begin{cases} \frac{f_{i+1,j}-2f_{ij}+f_{i-1,j}}{h^2} = (G_{11})_{ij} \frac{f_{i+1,j}-f_{i-1,j}}{2h} + (G_{11}^2)_{ij} \frac{f_{ij+1}-f_{ij-1}}{2h} + \frac{L_{ij}}{\sqrt{E_{ij}+G_{ij}-1}}, (x_i,y_j) \in \Omega \cap \partial\Omega \\ \frac{f_{i,j+1}-2f_{ij}+f_{i,j-1}}{h^2} = (G_{22})_{ij} \frac{f_{i+1,j}-f_{i-1,j}}{2h} + (G_{22}^2)_{ij} \frac{f_{ij+1}-f_{ij-1}}{2h} + \frac{N_{ij}}{\sqrt{E_{ij}+G_{ij}-1}}, (x_i,y_j) \in \Omega \cap \partial\Omega \end{cases} \quad (1)$$

where E, F, G, L, N are the first and second fundamental coefficients of a surface, these finite differences can be expressed as,

$$E_{ij} \approx 1 + \left(\frac{\tilde{f}_{i+1,j}-\tilde{f}_{i-1,j}}{2h} \right)^2 \quad (2)$$

$$F_{ij} \approx \left(\frac{\tilde{f}_{i+1,j}-\tilde{f}_{i-1,j}}{2h} \right) \left(\frac{\tilde{f}_{ij+1}-\tilde{f}_{ij-1}}{2h} \right) \quad (3)$$

$$G_{ij} \approx 1 + \left(\frac{\tilde{f}_{ij+1}-\tilde{f}_{ij-1}}{2h} \right)^2 \quad (4)$$

$$L_{ij} \approx \frac{\tilde{f}_{i+1,j}-2\tilde{f}_{ij}+\tilde{f}_{i-1,j}}{h^2} \sqrt{1 + \left(\frac{\tilde{f}_{i+1,j}-\tilde{f}_{i-1,j}}{2h} \right)^2 + \left(\frac{\tilde{f}_{ij+1}-\tilde{f}_{ij-1}}{2h} \right)^2} \quad (5)$$

$$N_{ij} \approx \frac{\tilde{f}_{i,j+1}-2\tilde{f}_{ij}+\tilde{f}_{i,j-1}}{h^2} \sqrt{1 + \left(\frac{\tilde{f}_{i+1,j}-\tilde{f}_{i-1,j}}{2h} \right)^2 + \left(\frac{\tilde{f}_{ij+1}-\tilde{f}_{ij-1}}{2h} \right)^2} \quad (6)$$

The finite difference of Γ_k^l ($k=11, 22; l=1, 2$) can be formulated as,

$$(\Gamma_{11}^1)_{ij} \approx \frac{G_{ij}(E_{i+1,j}-E_{i-1,j})-2F_{ij}(F_{i+1,j}-F_{i-1,j})+F_{ij}(E_{ij+1}-E_{ij-1})}{4(E_{ij}G_{ij}-F_{ij}^2)h} \quad (7)$$

$$(\Gamma_{11}^2)_{ij} \approx \frac{2E_{ij}(F_{i+1,j}-F_{i-1,j})-E_{ij}(E_{ij+1}-E_{ij-1})-F_{ij}(E_{i+1,j}-E_{i-1,j})}{4(E_{ij}G_{ij}-F_{ij}^2)h} \quad (8)$$

$$(\Gamma_{22}^1)_{ij} \approx \frac{2G_{ij}(F_{ij+1}-F_{ij-1})-G_{ij}(G_{i+1,j}-G_{i-1,j})-F_{ij}(G_{ij+1}-G_{ij-1})}{4(E_{ij}G_{ij}-F_{ij}^2)h} \quad (9)$$

$$(\Gamma_{22}^2)_{ij} \approx \frac{E_{ij}(G_{ij+1}-G_{ij-1})-2F_{ij}(F_{ij+1}-F_{ij-1})+F_{ij}(G_{i+1,j}-G_{i-1,j})}{4(E_{ij}G_{ij}-F_{ij}^2)h} \quad (10)$$

where h is grid space, $(x_i, y_j) \in \Omega \cap \partial\Omega$ is a point in the computational domain Ω , $f_{ij} = g_{ij}(x_i, y_j) \in \partial\Omega$ is boundary value; $f_{ij} = \tilde{f}_{ij}$, $(x_i, y_j) \in \Phi \subset \Omega$, Φ are sampling data, \tilde{f}_{ij} is interpolation value in terms of the sampling values of \tilde{f}_{ij} , $(x_i, y_j) \in \Phi \subset \Omega$.

The matrix formulation of SMTS can be expressed as,

$$\begin{cases} B_1 f^{n+1} = l_1^n \\ B_2 f^{n+1} = l_2^n \end{cases} \quad (11)$$

where, B_1 and B_2 represent coefficient matrices of equation (1), respectively; l_1^n and l_2^n represent the right-hand vectors of equation (1), respectively; $f^{n+1} = [f_{1,1}^{n+1}, f_{1,2}^{n+1}, \dots, f_{1,Mx}^{n+1}, f_{2,1}^{n+1}, f_{2,2}^{n+1}, \dots, f_{2,Mx}^{n+1}, \dots, f_{My,1}^{n+1}, f_{My,2}^{n+1}, \dots, f_{My,Mx}^{n+1}]^T$, $Mx+2$ and $My+2$ represent the number of grid cells in the x and y directions, respectively.

Suppose one sampling point is located at the lattice (x_i, y_j) in the computational domain Ω , the interpolation value should be equal or approximate to the sampling value at this lattice, so a constrained equation is added to the Eq. (11) and the formulation of SMTS can be expressed as,

$$\begin{cases} \min \|Bf^{n+1} - l^n\|_2 \\ \text{s.t. } Mf^{n+1} = h \end{cases} \quad (12)$$

where $B = \begin{bmatrix} B_1 \\ B_2 \end{bmatrix}$, $l^n = \begin{bmatrix} l_1^n \\ l_2^n \end{bmatrix}$, M represents the coefficient matrix of sampling data, h represents the vector of sampling value.

Considering sufficiently large λ , SMTS formulation can be transformed to the expression as,

$$\min_f \left\| \begin{bmatrix} B \\ \lambda M \end{bmatrix} f^{n+1} - \begin{bmatrix} l^n \\ \lambda h \end{bmatrix} \right\|_2 \quad (13)$$

Or

$$Sf^{n+1} = t^n \tag{14}$$

where $S = [B^T \quad \lambda M^T] \begin{bmatrix} B \\ \lambda M \end{bmatrix}$, $t^n = [B^T \quad \lambda M^T] \begin{bmatrix} I^n \\ \lambda h \end{bmatrix}$. Therefore, the computational results of a DEM can be expressed as,

$$f^{n+1} = S^{-1}t^n \tag{15}$$

The parameter λ is the weight of the sampling points and determines the contribution of the sampling points to the simulated surface. λ is a real number or an element, which means all sampling points have the same weight or different weights. In a complex region, area affected by a sampling point is smaller than in a flat region. Therefore, a smaller value of λ is selected in a complex region and a bigger value is selected in a flat region.

Based on the above fundamental theory, a DEM can be generated by the following procedures:

- (1) Conducting interpolation on the computational domain Ω in terms of sampling data, from which we can get interpolated approximate values of the simulated grids.
- (2) Computing the first and second fundamental coefficients of SMTS.
- (3) Calculating Γ_k^l ($k=11, 12, 22; l=1, 2$), S and t^n , respectively.
- (4) Solving Eq. (15).
- (5) Repeating (2)–(4) until the simulation results meet the pre-set accuracy. The accuracy controller can be set as $\max(|f_{ij}^n - f_{ij}^{n+1}|) \leq \varepsilon$, where ε is an accuracy tolerance.

3. ETR

3.1. The concept of ETR

DEM's can be generated using different interpolation methods (Fisher, 1998; Goodchild and Gopal, 1989). DEM accuracy tells how faithfully the generated DEM represents the true ground (Thebald, 1989). DEM error can be defined as the elevation difference between the constructed DEM and the corresponding true surface (Fisher, 1993). This definition has been accepted as a general understanding of DEM error. DEM sampling and interpolation errors mean the elevation difference between DEM grid lattices obtained from sampling and interpolation techniques and the corresponding points on the true ground (Tang, 2000). If all the sampling and interpolation grids have no errors and the DEM resolution is infinitely small, the DEM can be regarded as the true ground surface. However, because of the limitations of computer processing and storage ability, etc, it is impossible to make the DEM resolution as high as possible. Therefore, no matter how small the sampling and interpolation errors are, the derived DEM is only an approximation to the real-world ground. The information loss is due purely to the finite grid interval and using linear representation for a terrain surface (Huang, 2000). The elevation discrepancy between the DEM and the true ground surface is termed DEM ETR that increases as the resolution and terrain roughness increases. Thus, ETR is considered as a measure of DEM fidelity and total DEM errors are actually composed of not only sampling and interpolation errors but also ETRs.

3.2. The algorithm of calculating ETR

Fig. 1 describes the existence of ETR on a 2D profile. The thick line \overline{ABC} represents the true ground surface, while A and C are two adjacent elevation points, free from sampling and interpolation

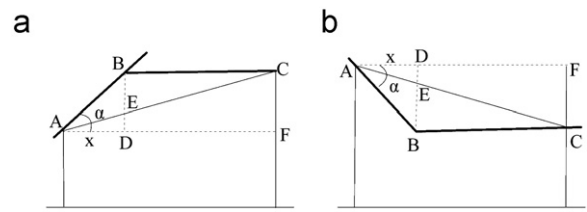


Fig. 1. A 2D profile model describing ETR: (a) Point B is above \overline{AC} (b) Point B is below \overline{AC} .

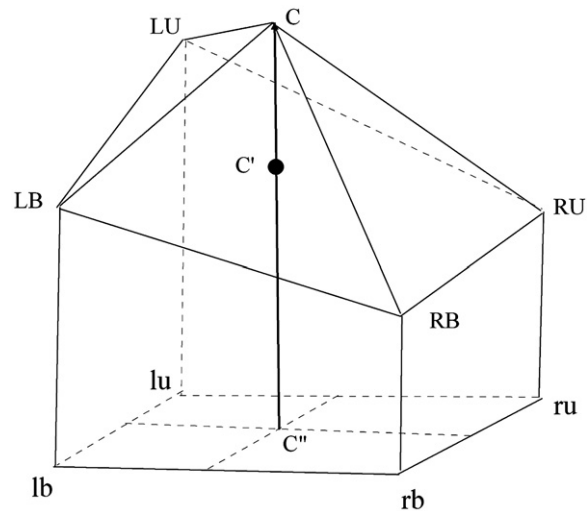


Fig. 2. A 3D DEM describing ETR.

errors. Because of the linear representation of the true ground surface with A and C , there exists a discrepancy between \overline{AC} and \overline{ABC} . Suppose α represents the slope at A , and x is a variable, representing the distance between A and D , ETR of \overline{BE} can be formulated as,

$$\overline{BE} = \overline{BD} - \overline{ED} = x \tan \alpha - \frac{x^2 \tan \alpha}{d} \tag{16}$$

where d represents DEM resolution.

Letting one derivative of \overline{BE} be equal to zero, we can obtain the position of D , where \overline{BE} has the biggest value.

$$\frac{d(\overline{BE})}{dx} = \tan \alpha - \frac{2x \tan \alpha}{d} = 0; \quad x = \frac{d}{2} \tag{17}$$

Eq. (17) indicates that at the middle point of \overline{AF} , it would be most possible to get the maximum ETR. In terms of this analysis, the maximum ETR between A and C can be expressed as,

$$Etr_{\max} = H_B - \frac{H_A + H_C}{2} \tag{18}$$

where, H_A , H_B and H_C represent the elevation values at A , B and C , respectively.

Eq. (18) indicates that when point B is above \overline{AC} , Etr_{\max} is positive (Fig. 1a), and when point B is below \overline{AC} , Etr_{\max} is negative (Fig. 1b).

Let us extend the ETR to a 3D DEM:

As illustrated in Fig. 2, lu, lb, rb, ru is a regular DEM grid, C' is the center of the grid; LU, LB, RB, RU and C are the points on the ground surface; $H_{LU}, H_{LB}, H_{RU}, H_{RB}$ and H_C are the corresponding elevations at LU, LB, RU, RB and C , respectively. By the same principle discussed above, the maximum ETR within a grid can be

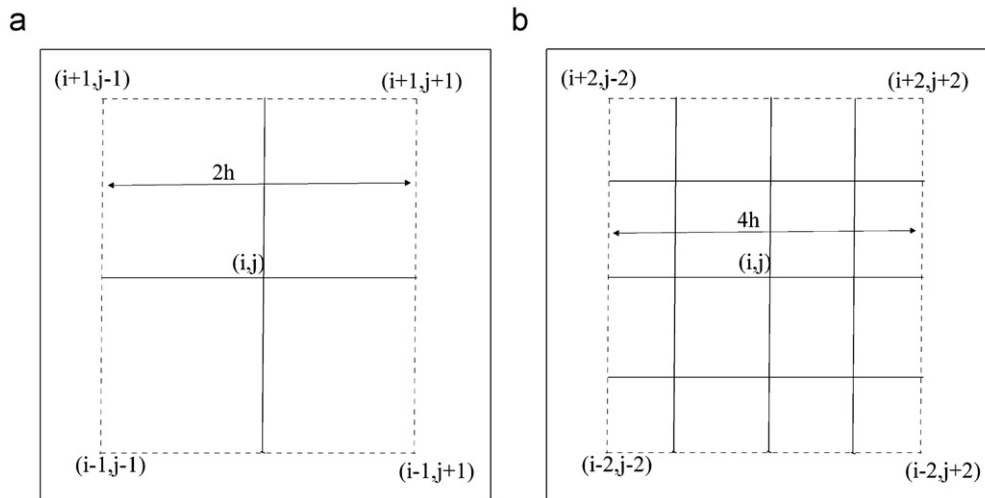


Fig. 3. Kernel windows used to calculate ETRs of a DEM: (a) A 3×3 kernel window and (b) a 5×5 kernel window.

expressed as,

$$Etr_{\max} = H_C - \frac{H_{LU} + H_{LB} + H_{RB} + H_{RU}}{4} \quad (19)$$

Assuming a DEM resolution is h , a 3×3 kernel window is employed to calculate the maximum ETR of every lattice with formula (20). When the window moves through the whole DEM cell by cell and calculates the ETR value of each cell, we can derive an expected ETR matrix with the resolution of $2h$ (Fig. 3a).

$$Etr_{i,j} = H_{i,j} - \frac{H_{i+1,j+1} + H_{i+1,j-1} + H_{i-1,j-1} + H_{i-1,j+1}}{4} \quad (20)$$

If the kernel window is extended to 5×5 , 7×7 ..., a set of DEM ETRs with the resolutions of $4h$, $6h$... can be computed respectively (Tang, 2000) (Fig. 3b). Under a certain resolution, the root mean square error (RMSE) of ETR matrix ($RMSE_{ETR}$) as an error index at a global level is calculated as follows:

$$RMSE_{ETR} = \sqrt{\frac{\sum_{i=1, j=1}^{i=Row, j=Column} Etr_{i,j}^2}{Row \times Column}} \quad (21)$$

where, *Row* and *Column* represent the row and column of ETR matrix, respectively.

3.3. Total DEM error

From what have been discussed above, it can be concluded that in a DEM, total DEM errors are actually composed of, not only sampling and interpolation errors, but also ETRs. Sampling and interpolation errors may be caused by the limitation of sampling and interpolation technologies, computer processing, storage ability, etc. ETR is caused by the DEM resolution and the complexity of a region. Root mean square error (RMSE) which provides an accuracy index at a global level (Burrough, 1986; Holmes et al., 2000) can be used to estimate the effect of sampling and interpolation errors on a DEM (Wechsler and Kroll, 2006). The RMSE is expressed as,

$$RMSE = \sqrt{\frac{\sum_{i=1}^N (f_i - sf_i)^2}{N}} \quad (22)$$

where, N represents the number of validation points; sf_i refers to the i th simulated or interpolated elevation, and f_i represents the i th known or measured elevation.

Therefore, based on the error propagation theorem, total DEM error in terms of RMSE ($RMSE_{ETD}$) can be formulated as,

$$RMSE_{ETD} = \sqrt{RMSE_{ESI}^2 + RMSE_{ETR}^2} \quad (23)$$

where, $RMSE_{ESI}$ refers to sampling and interpolation errors in terms of RMSE, which can be computed with formula (22); $RMSE_{ETR}$ represents ETR in terms of RMSE, which can be computed with formula (21).

Above all, total DEM error including not only sampling and interpolation errors but also ETR can be regarded as a good criterion for comprehensively assessing DEM accuracy at a global level.

4. Numerical and real-world tests

4.1. Comparative analysis

In addition to the newly developed SMTS, there are many classical interpolation methods including IDW, SPLINE and KRIGING (Blomgren, 1999; Ries, 1993; Robinson, 2006), with which the performance of SMTS can be compared. In this paper, all the classical interpolation methods were performed using the module of 3D analyst in ARCGIS 9.1 with the default parameters. For IDW, the power is 2, the search radius is variable and the maximum number of the researched points is 12. For SPLINE, the REGULARIZED option is used, the weight is 0.1, and the number of the researched points is 12. For KRIGING, ordinary method is selected, the model of semivariogram is spherical, the searched radius is variable, and the maximum number of the searched points is 12.

4.2. A numerical test

The canonical surface $z = 2\sin(\pi x)\sin(\pi y) + 1$ (Fig. 4) was taken as the test surface, so that the 'true' output value can be pre-determined to avoid uncertainty caused by uncontrollable data errors. Its computational domain is $[0,1] \times [0,1]$. The RMSEs of ETR matrixes ($RMSE_{ETRs}$) of different resolutions were calculated with formulas (20) and (21). The regression model that relates $RMSE_{ETR}$ to resolution was generated with SPSS14.0 (formula (24)), and the relationship appears to have a non-linear (quadratic) correlation (Fig. 5).

$$RMSE_{ETR} = 1.57 \times 10^{-6} - 0.001h + 2.516h^2; \quad R^2 = 1 \quad (24)$$

where h represents resolution.

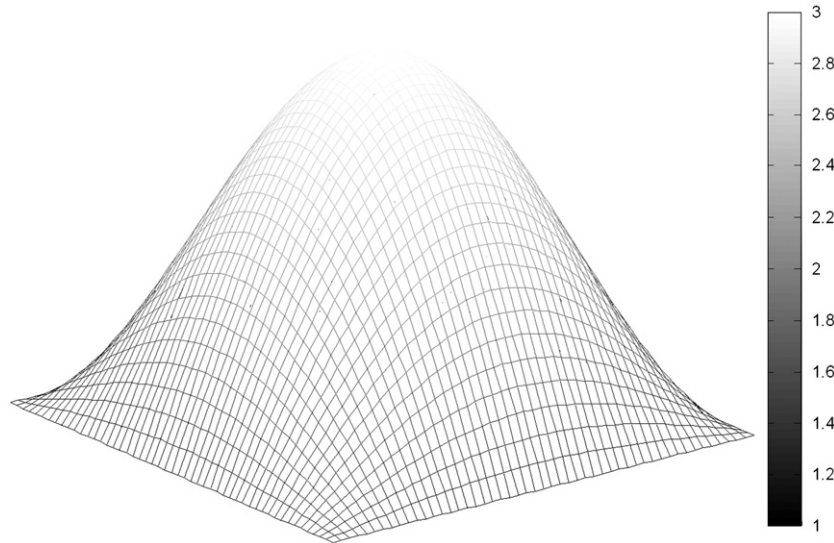


Fig. 4. Canonical surface.

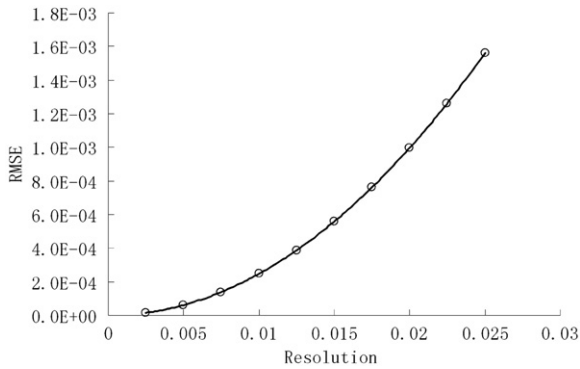


Fig. 5. Regression model relating $RMSE_{ETR}$ to resolution of canonical surface.

Table 1
 $RMSE_{ESI}$ s of the four interpolation methods of canonical surface.

Resolution	SMTS ($\times 10^{-4}$)	IDW	SPLINE	KRIGING
1/8	9.72	0.35	0.21	0.37
1/16	5.61	0.45	0.29	0.51
1/32	3.67	0.53	0.34	0.58
1/64	4.57	0.57	0.36	0.62

In the computational domain $[0,1] \times [0,1]$, 25 points were evenly sampled from the canonical surface to construct DEMs by SMTS and the classical interpolators with the resolutions of 1/8, 1/16, 1/32 and 1/64. Because these 25 points are free from sampling errors, $RMSE_{ESI}$ only refers to interpolation error without sampling error. The $RMSE_{ESI}$ s were calculated with formula (22) (Table 1).

Irrespective of the resolution, SMTS is much more accurate than the classical interpolation methods (Tables 1 and 2). The resolution of 1/8 gives SMTS the lowest accuracy. However, the accuracy of SMTS is still 360.1, 216 and 380.7 times higher than those of IDW, SPLINE and KRIGING, respectively (Table 2). Under the resolution of 1/32, SMTS has the highest accuracy, which is 1444.1 times higher than that of IDW, 926.4 times higher than that of SPLINE and 1580.4 times higher than that of KRIGING (Table 2).

Table 2
Ratio of $RMSE_{ESI}$ of a classical interpolation method to that of SMTS of canonical surface.

Resolution	IDW	SPLINE	KRIGING
1/8	360.1	216.0	380.7
1/16	802.1	516.9	909.1
1/32	1444.1	926.4	1580.4
1/64	1247.3	787.7	1356.7

Table 3
 $RMSE_{ETD}$ s of the four interpolation methods of canonical surface.

Resolution	SMTS ($\times 10^{-4}$)	IDW	SPLINE	KRIGING
1/8	392	0.35	0.21	0.37
1/16	98	0.45	0.29	0.51
1/32	25	0.53	0.34	0.58
1/64	8	0.57	0.36	0.62

Table 4
Ratio of $RMSE_{ETD}$ of a classical interpolation method to that of SMTS of canonical surface.

Resolution	IDW	SPLINE	KRIGING
1/8	8.9	5.4	9.4
1/16	45.9	29.6	52.0
1/32	212.0	136.0	232.0
1/64	712.5	450.0	775.0

Total DEM errors in terms of RMSE ($RMSE_{ETD}$ s) were computed based on formula (23) and the results are shown in Table 3.

In terms of $RMSE_{ETD}$, the simulation results of SMTS are still more accurate than the classical interpolation methods, but ETR has a worse influence on the accuracy of SMTS than those of the classical interpolation methods (Tables 3 and 4). For example, in terms of $RMSE_{ESI}$ (Table 2), under the resolution of 1/16, the SMTS accuracy is 802.1, 516.9 and 909.1 times higher than those of IDW, SPLINE and KRIGING, respectively. But SMTS is only 45.9 times higher than that of IDW, 29.6 times of SPLINE and 52 times of KRIGING in terms of $RMSE_{ETD}$ under the same resolution (Table 4).

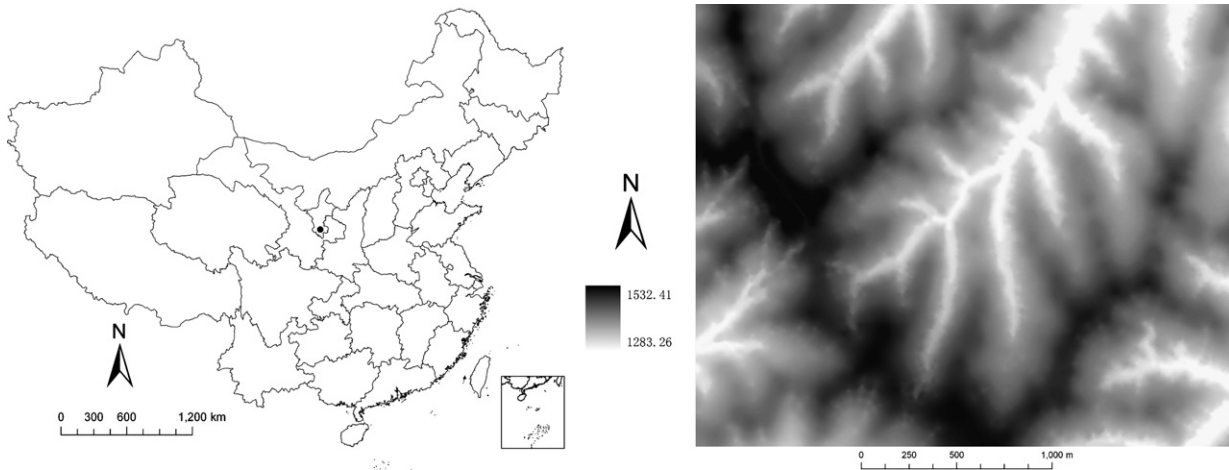


Fig. 6. Location and topography of Dongzhi tableland.

Under the resolution of 1/64 (Table 1), the $RMSE_{ESI}$ of SMTS is bigger than that of the resolution of 1/32. But when taking the ETR into account (Table 3), the $RMSE_{ETD}$ of SMTS becomes smaller and smaller with the resolution increasing, which indicates that, ETR becomes a dominant component of the SMTS errors. Considering all the DEMs derived from the classical interpolation methods, the $RMSE_{ETD}$ increases with the increasing resolution.

Above all, SMTS is much more accurate than the classical interpolation methods, and the total DEM error can give interpolation methods a more comprehensive accuracy evaluation than the sampling and interpolation errors at a global level.

4.3. A real-world example

The Dongzhi tableland located in Gansu province, China was selected as a real-world test region (Fig. 6). The geographic coordinates of its central point is $107.88^{\circ}E$ and $36.03^{\circ}N$. Its elevation varies from 1283 to 1532 m. Its slope varies from 1° to 85° .

The topographic map covering the research region with a scale of 1:5000 and the contour interval of 25 m was scanned. The topographic map was enlarged three times to enhance the digitization accuracy. Contours were traced using the editor module in ARCGIS 9.1 with elevations as identification labels. The density of sampled elevations was based on the sinuosity of contour lines. Hence, more elevations were sampled at sections with a sharp curvature. The Gauss–Krueger projection, in which each zone is 3° of longitude in width, was adopted to transform Beijing geographical coordinates established in 1954 into rectangular Cartesian coordinates for easier calculation and Dongzhi tableland was projected to the 36th zone. The Huang-Hai Elevation System established in 1956 was adopted as an elevation datum. After the transformation of the coordinate system, the elevation points of contour lines were transformed into scattered points with the information of coordinates using the Data Management Tools module in ARCGIS 9.1.

All the points were used to construct a 5 m DEM, which was used to calculate the ETR matrices with the kernel windows of different resolutions from 10 to 100 m with the step interval of 10 m. The $RMSE_{ETRS}$ were computed to obtain the regression model relating $RMSE_{ETRS}$ to DEM resolutions. The regression model was generated with SPSS14.0 (formula (25)), and the relationship appears to have a linear correlation (Fig. 7).

$$RMSE_{ETR} = 0.134h + 1.737; \quad R^2 = 1 \quad (25)$$

where, h represents resolution.

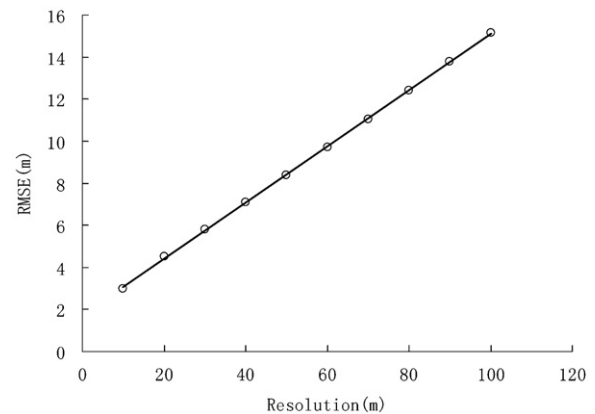


Fig. 7. Regression model relating $RMSE_{ETR}$ to resolution in Dongzhi tableland.

Table 5

$RMSE_{ESI}$ s of the four interpolators in Dongzhi tableland (m).

Resolution	SMTS	IDW	SPLINE	KRIGING
30	9.33	13.72	13.05	13.96
20	9.60	11.79	10.41	12.64
10	8.86	11.14	9.69	12.28
5	8.79	10.80	9.18	12.15

Table 6

Ratio of $RMSE_{ESI}$ of a classical interpolator to that of SMTS in Dongzhi tableland

Resolution	IDW	SPLINE	KRIGING
30	1.47	1.40	1.50
20	1.23	1.08	1.32
10	1.26	1.09	1.39
5	1.23	1.04	1.38

All the scattered elevation points from the contour map were randomly divided into two groups: one group containing 70% of the elevations used for DEM generation, the other group for DEM validation. Based on the elevations used for DEM construction, DEMs with the resolutions of 5, 10, 20 and 30 m were generated with SMTS and the three classical interpolation methods. The $RMSE_{ESI}$ of each DEM was calculated with the validation points (Table 5).

Irrespective of the DEM resolution, SMTS is more accurate than the classical interpolators (Table 5). However, the accuracy difference is less distinct than the case of the numerical test. For

Table 7
RMSE_{ETD}s of the four interpolators in Dongzhi tableland (m).

Resolution	SMTS	IDW	SPLINE	KRIGING
30	10.97	14.88	14.26	15.10
20	10.56	12.59	11.30	13.39
10	9.40	11.56	10.16	12.67
5	9.11	11.06	9.49	12.39

Table 8
Ratio of RMSE_{ETD} of a classical interpolator to that of SMTS in Dongzhi tableland.

Resolution	IDW	SPLINE	KRIGING
30	1.36	1.30	1.38
20	1.19	1.07	1.27
10	1.23	1.08	1.35
5	1.21	1.04	1.36

example, compared with the classical interpolation methods, the resolution of 30 m gives SMTS the highest accuracy (Table 6), which is only 1.47 times higher than that of IDW, 1.40 times of SPLINE, and 1.50 times of KRIGING. The accuracy loss may be caused by location differences between the sampling points and the corresponding central points of lattices of the simulated surfaces (Yue and Song, 2008).

The RMSE_{ETD}s were calculated with formula (23) (Table 7).

Irrespective of the resolution, SMTS is more accurate than the classical interpolation methods in terms of RMSE_{ETD} (Tables 7 and 8). Column 2 of Table 5 indicates that the resolution of 20 m gives SMTS a higher accuracy loss than other resolutions. But when taking the ETR into account (Table 7), the RMSE_{ETD} of SMTS decreases as the resolution increases. Therefore, ETR plays an important role in the accuracy evaluation.

All the shaded relief maps of the simulated DEM with the resolution of 10 m were constructed using the four interpolators to represent the terrain relief of the Dongzhi tableland (Fig. 8). These maps were made with the same azimuth and altitude angles of the default values in ARCGIS 9.1. The Azimuth angle of the light source is expressed in positive degrees from 0° to 360°, measured clockwise from the north. The default is 315°.

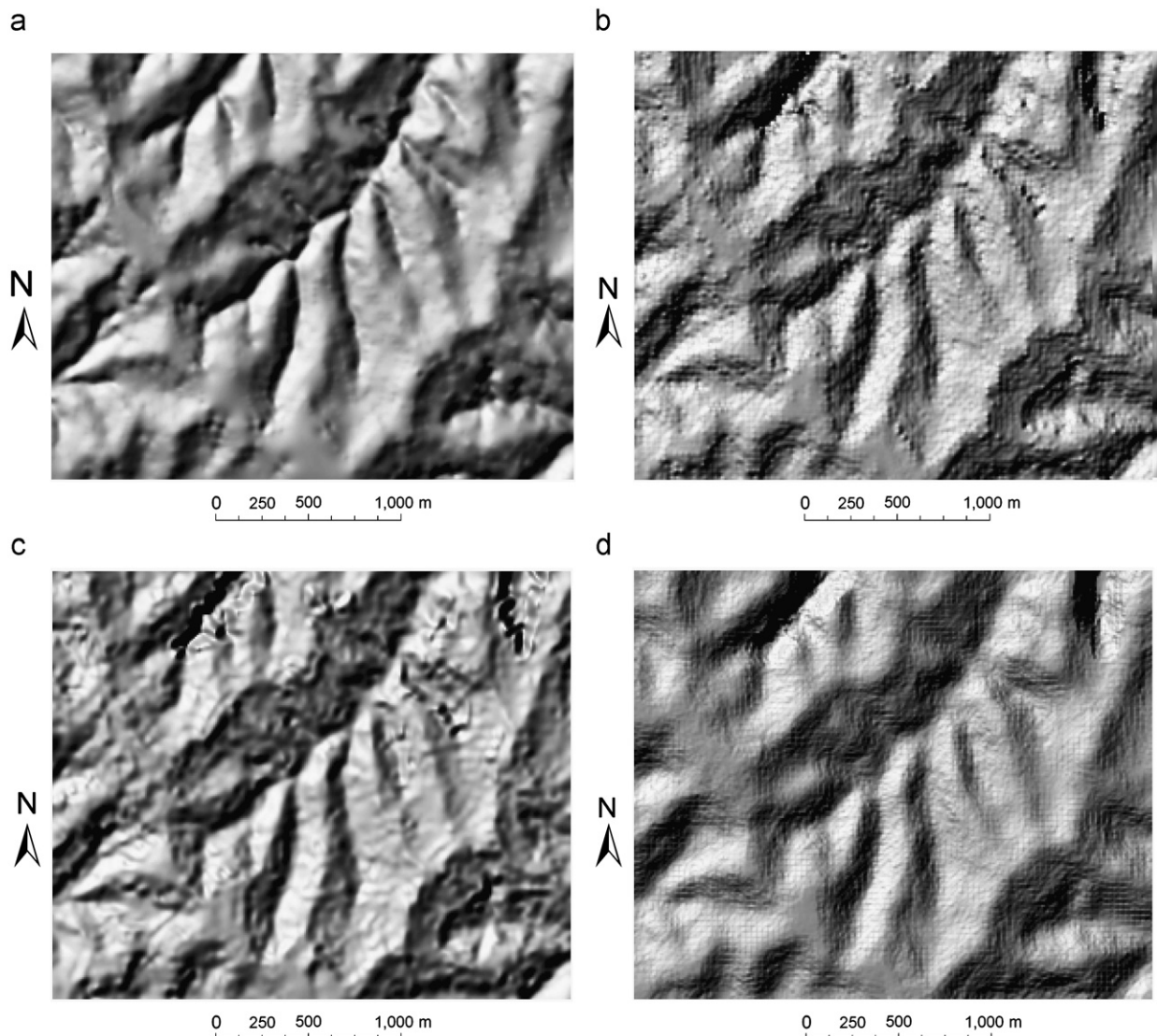


Fig. 8. 3D shaded relief maps of SMTS and the classical interpolation methods in Dongzhi tableland: (a) SMTS (b) IDW (c) SPLINE (d) KRIGING.

The Altitude angle of the light source above the horizon is expressed in positive degrees, with 0° at the horizon and 90° directly overhead. The default is 45° .

The 3D shaded relief maps indicate that SMTS has a much better simulation result than those of the classical interpolation methods (Fig. 8a). The simulation result of the IDW has many abrupt changes in slope obtained from changes in shades of grays, and is coarser than that of SMTS (Fig. 8b). The SPLINE method is significantly influenced by an oscillation problem, especially in the right bottom area (Fig. 8c). The KRIGING simulation result has many wrinkles and an obvious peak truncation and pit-fill problem (Fig. 8d).

From what have been discussed above, it can be concluded that SMTS is more accurate than the classical interpolation methods and it may be regarded as an alternative interpolator for DEM construction.

5. Conclusions and discussion

The concept and the computation of ETR are presented and total DEM error is computed in terms of the error propagation theorem. Both the numerical test and the real-world example indicate that SMTS has a higher accuracy than the classical interpolation methods including IDW, SPLINE and KRIGING performed in ARCGIS 9.1 in terms of $RMSE_{ESI}$ and of $RMSE_{ETD}$. In the numerical test, the ETR has a worse influence on the accuracy of SMTS than those of the classical interpolators. In the real-world example, although SMTS is more accurate than other interpolators, there is a big accuracy loss compared with the numerical test, which may be caused by location differences between the sampling points and the corresponding central points of lattices of the simulated surfaces. Total DEM error including not only sampling and interpolation errors but also ETR is considered as a good criterion for DEM accuracy evaluation at a global level.

In addition to presenting a better accuracy assessment of the DEM product, ETR enables a DEM user to select an appropriate grid interval for sampling and interpolation based on the ETRs of a range of grid intervals. Thus, it is recommended that when constructing DEM, the producer should provide the ETRs of several candidate grid intervals for user's choice and assessment.

SMTS must use an equation set to simulate each lattice of a surface and DEM construction based on SMTS is eventually transformed to solve a large sparse linear system (Yue et al., 2008). The traditional direct methods for solving the linear system indicate that the SMTS computational time is approximately proportional to the third power of the total number of grid cells in the computational domain (Saad, 2003; Davis, 2006), which seriously hampers its use in a broad number of applications. An adaptive mesh refinement algorithm can select a resolution that is as coarse as possible while still meeting a defined accuracy to serve a specific purpose (Berger, 1989; Trottenberg et al., 2001). Thus future work is focused on the establishment of an adaptive algorithm of SMTS to reduce its data volume and computational demands.

Acknowledgments

Special thanks go to the two anonymous reviewers for their assistance, comments and suggestions. This work is supported by China National Science Fund for Distinguished Young Scholars (40825003) and by Free Research Project of State Key Laboratory of Resources and Environment Information System (081105), by National Key Technologies R&D Program of Ministry of Science and Technology of the People's Republic of China (2006BAC08B), by National High-Tech R&D Program of Ministry of Science and Technology of the People's Republic of China (2006AA12Z219),

and by Doctoral Candidate Innovation Research Support Program by Science & Technology Review (kjdb200902-3).

References

- Aguilar, F.J., Aguilar, M.A., Agera, F., 2007. Accuracy assessment of digital elevation models using a non-parametric approach. *International Journal of Geographical Information Science* 21, 667–686.
- Armstrong, R.N., Martz, L.W., 2003. Topographic parameterization in continental hydrology: a study in scale. *Hydrological Processes* 17, 3763–3781.
- Berger, M.J., 1989. Local adaptive mesh refinement for shock hydrodynamics. *Journal of Computational Physics* 82, 64–84.
- Blomgren, S., 1999. A digital elevation model for estimating flooding scenarios at the Falsterbo Peninsula. *Environmental Modelling and Software* 14, 579–587.
- Bolstad, P.V., Stowe, T., 1994. An evaluation of DEM accuracy: elevation, slope and aspect. *Photogrammetric Engineering and Remote Sensing* 60, 1327–1332.
- Bonk, R., 2007. Scale-dependent effect of input data design on DEM accuracy. In: Peckham, R.J., Jordan, G. (Eds.), *Digital Terrain Modelling: Development and Applications in a Policy Support Environment*. Springer, Berlin, pp. 83–98.
- Burrough, P.A., 1986. *Principles of Geographical Information Systems for Land Resources Assessment*. Oxford University Press, New York, 220pp.
- Carlisle, B.H., 2005. Modelling the spatial distribution of DEM error. *Transactions in GIS* 9, 521–540.
- Carrara, G., Bitelli, A., Carla, R., 1997. Comparison of techniques for generating digital terrain models from contour lines. *International Journal of Geographical Information Science* 11, 451–473.
- Carter, J., 1990. Some effects of spatial resolution in the calculation of slope using the spatial derivative. In: *Proceeding of the 1990 ACSM-ASPRS Annual Convention*, Denver, CO, pp. 43–52.
- Chang, K.T., Tsai, B.W., 1991. The effect of DEM resolution on slope and aspect mapping. *Cartography and Geographic Information Society* 9, 69–77.
- Chaplot, V., Darboux, F., Bourennane, H., Legu dois, S., Silvera, N., Phachomphon, K., 2006. Accuracy of interpolation techniques for the derivation of digital elevation models in relation to landform types and data density. *Geomorphology* 77, 126–141.
- Davis, T.J., 2006. *Direct Methods for Sparse Linear Systems* 1st edn. SIAM, Philadelphia, 217pp.
- Erdogan, S., 2009. A comparison of interpolation methods for producing digital elevation models at the field scale. *Earth Surface Processes and Landforms* 34, 366–376.
- Fisher, P.F., 1993. Algorithm and implementation uncertainty in viewshed analysis. *International Journal of Geographical Information Science* 7, 331–347.
- Fisher, P.F., 1998. Improved modeling of elevation error with geostatistics. *Geoinformatica* 2, 215–233.
- Fisher, P.F., Tate, N.J., 2006. Causes and consequences of error in digital elevation models. *Progress in Physical Geography* 30, 467–489.
- Gao, J., 1997. Resolution and accuracy of terrain representation by grid DEMs at a micro-scale. *International Journal of Geographical Information Science* 11, 199–212.
- Gao, J., 1998. Impact of sampling intervals on the reliability of topographic variables mapped from grid DEMs at a micro-scale. *International Journal of Geographical Information Science* 12, 875–890.
- Goodchild, M.F., Gopal, S. (Eds.), 1989. *The Accuracy of Spatial Databases* 1st edn. CRC Press, New York.
- Gray, A., Abbena, E., Salamon, S. (Eds.), 2006. *Modern Differential Geometry of Curves and Surfaces with Mathematica* 3rd edn. CRC Press, New York.
- Henderson, D.W. (Ed.), 1998. *Differential Geometry: A Geometric Introduction* 1st edn. Prentice Hall, New Jersey, USA.
- Holmes, K.W., Chadwick, O.A., Kyriakidis, P.C., 2000. Error in a USGS30-meter digital elevation model and its impact on terrain modeling. *Journal of Hydrology* 233, 154–173.
- Huang, Y.D., 2000. Evaluation of information loss in digital elevation models with digital photogrammetric systems. *Photogrammetric Record* 16, 781–791.
- Huang, Z., Lees, B., 2005. Representing and reducing error in natural-resource classification using model combination. *International Journal of Geographical Information Science* 19, 603–621.
- Liseikin, V.D., 2004. *A Computational Differential Geometry Approach to Grid Generation* 2nd edn. Springer, Berlin, 308pp.
- L pez, C., 1997. Locating some types of random errors in Digital Terrain Models. *International Journal of Geographical Information Science* 11, 677–698.
- Polidori, L., Chorowicz, J., Guillande, R., 1991. Description of terrain as a fractal surface, and application to digital elevation model quality assessment. *Photogrammetric Engineering and Remote Sensing* 57, 1329–1332.
- Rees, W.G., 2000. The accuracy of Digital Elevation Models interpolated to higher resolutions. *International Journal of Remote Sensing* 21, 7–20.
- Ries, L., 1993. Areas of influence for IDW-interpolation with isotropic environmental data. *Catena* 20, 199–205.
- Robinson, T.P., 2006. Testing the performance of spatial interpolation techniques for mapping soil properties. *Computers and Electronics in Agriculture* 50, 97–108.
- Saad, Y., 2003. *Iterative Methods for Sparse Linear Systems* 2nd edn. Society for Industrial Mathematics, Philadelphia, 528pp.
- Schut, G., 1976. Review of interpolation methods for digital terrain models. *The Canadian Surveyor* 30, 389–412.

- Skidmore, A.K., 1989. A comparison of techniques for calculating gradient and aspect from a gridded digital elevation model. *International Journal of Geographical Information Science* 4, 323–334.
- Tang, G.A., 2000. A Research on the Accuracy of Digital Elevation Models. Science Press, Beijing New York, 165pp.
- Thebald, D.M., 1989. Accuracy and bias issues in surface representation. In: Goodchild, M.F., Gopal, S. (Eds.), *The Accuracy of Spatial Databases*. CRC Press, New York, pp. 99–106.
- Trottenberg, U., Oosterlee, C., Schuller, A., 2001. *Multigrid* 1st edn. Academic Press, London, 631pp.
- Walsh, S., Lightfoot, D., Butler, D., 1987. Recognition and assessment of error in geographic information systems. *Photogrammetric Engineering and Remote Sensing* 53, 1423–1430.
- Wechsler, S.P., Kroll, C.N., 2006. Quantifying DEM uncertainty and its effect on topographic parameters. *Photogrammetric Engineering and Remote Sensing* 72, 1081–1091.
- Wise, S., 1998. The effect of GIS interpolation errors on the use of digital elevation models in geomorphology. In: Lane, S., Richards, K., Chandler, J. (Eds.), *Landform Monitoring, Modelling and Analysis*. John Wiley and Sons, New York, pp. 139–164.
- Yue, T.X., Du, Z.P., Song, D.J., 2007. A new method of surface modelling and its application to DEM construction. *Geomorphology* 91, 161–172.
- Yue, T.X., Du, Z.P., Song, Y.J., 2008. Ecological models: spatial models and geographic information systems. In: Jørgensen, S.E., Fath, B. (Eds.), *Encyclopedia of Ecology*. Elsevier Limited, England, pp. 3315–3325.
- Yue, T.X., Song, Y.J., 2008. The YUE-HASM method. In: *Proceeding of the eighth International Symposium on Spatial Accuracy Assessment in Natural Resources and Environmental Sciences*, Shanghai, pp. 148–153.
- Zhou, Q.M., Liu, X.J., 2004. Analysis of errors of derived slope and aspect related to DEM data properties. *Computers & Geosciences* 30, 369–378.